Nonlinear Dyn (2021) 103:1427–1438
https://doi.org/10.1007/s11071-020-06165-6

ORIGINAL PAPER

Cascaded essential nonlinearities for enhanced vibration suppression and energy harvesting

Yang Jin · Shuai Hou · Tianzhi Yang

Received: 15 May 2020 / Accepted: 15 December 2020 / Published online: 28 January 2021

Abstract The concept of simultaneous energy harvesting and vibration suppression has made tremendous progress in the past few years. However, the energy harvesting and vibration reduction seem to be independent, or even paradox in some scenarios; for example, energy harvesting strategy expects the primary system to maintain large-amplitude vibration as long as possible. In comparison, the vibration suppression strategy aims to suppress the vibration of primary system as soon as possible. In this paper, we aim to demonstrate how to properly design an integrated system, which first ensures the broadband vibration suppression performance, while at the same time, harvests additional energy as much as possible. To achieve this goal, a cascaded essentially nonlinear system is presented for high-sensitive vibration and harvesting energy. The presented device comprises a nonlinear energy sink and a nonlinear energy harvester with cascaded essential nonlinearities. Numerical results show that the presented device is able to simultaneously suppress vibration and harvest vibration energy over a wide frequency range. Moreover, unlike previous research, it is effective for extremely small initial impulses. This work explores possibilities for reducing and harvesting extremely low ambient vibration.

Keywords Nonlinear energy sink · Energy harvesting · Vibration suppression

Y. Jin
Tianjin Key Laboratory for Civil Aircraft Airworthiness and Maintenance, Civil Aviation University of China, Tianjin, China

S. Hou
School of Astronautics, Harbin Institute of Technology, Harbin, China

T. Yang (✉)
School of Mechanical Engineering and Automation, Northeastern University, Shenyang, China
e-mail: yang@dyn.tu-darmstadt.de

1 Introduction

Controlling and utilizing vibration energy has long been of interest of engineers; various vibration absorbers or tuned mass dampers (TMDs) were presented and commonly used. These devices rely on the linear resonance and thus are inherent narrowband; this limits the practical performance in broadband environment. Some possible solutions to improve the performance by using nonlinear resonance mechanism were proposed [1–4]. In 2001, the concept of nonlinear energy sink (NES) was presented [5, 6], serving as a powerful tool for triggering targeted energy transfer (TET) for various energy structures, which significantly improves the bandwidth due to the essential nonlinearity. Since then, the NES was

successfully applied to suppression vibration for various mechanical systems in a broadband [7–12].

On the other hand, the energy harvesting is another objective for absorbing excessive vibration energy; generally, an energy harvester expects the vibration amplitude of the primary system to remain in a high level. Similarly, for the vibration suppression problem, the broadband energy harvesting is of importance, which has been increasing the interest [13–22]. In Ref. [14], a bistable energy harvester incorporating essentially nonlinear stiffness was proposed, which is proved to be highly efficient and particularly sensitive to impulsive excitation. However, both the NES and NEH have a common limitation, that is, the initial energy threshold. Below that value, the NES or NES is ineffective because the influence of essential nonlinearity is small. This severely limits the application for vibration suppression and energy harvesting for low-amplitude vibration in ambient. Some researchers contributed to minimize the threshold; for example, Gendelman et al. [23] integrated two conventional NES and found that the threshold value of the combined NESs is greatly minimized. AL-Shudeifat [24] presented a new type of NES with negative and nonlinear stiffness, achieving a much higher efficiency and lower threshold. Wei et al. [25] reported a new mechanism for optimized targeted energy transfer, thus enabling an advanced NES with higher efficiency for all the values of pulse excitation.

The energy harvesting and vibration reduction seem to be independent, or even paradox in some scenarios, that is, energy harvesting strategy expects the primary system to maintain large-amplitude vibration as long as possible. In comparison, the vibration suppression strategy aims to suppress the vibration of primary system as soon as possible. Over the past few years, the idea of combining vibration isolator and energy harvester has been suggested in recent years. Kremer et al. [15] designed a NES energy harvester and achieved vibration suppression and energy harvesting in a broadband manner. Fang et al. [26] implemented a giant magnetostrictive energy harvester with a nonlinear energy sink for realizing TET. And these results were verified by the complexification-averaging (CX-A) technique [27]. Zhang et al. [28] presented a novel piezoelectric energy harvester with a nonlinear energy sink. However, the above works are based on single NES and the core idea of these works is to utilize the essential nonlinearity of NES for extending the bandwidth. Definitely, the combined NES and harvester can suppress the vibration and harvest energy simultaneously. However, the trade-off between vibration suppression and energy harvesting is not explored. In some scenario, for example, the vibration suppression is the primary task during the rocket launching mission. At the same time, it is expected to harvest the vibration as much as possible. When the NES is incorporated with a linear energy harvester, the vibration suppression performance is not ensured to be superior to a single NES. This inspires the objective of this paper. Unlike single NES, the cascading NES–NEH device is first designed to enhance vibration suppression and energy harvesting.

In this paper, we present a novel integrated device composed of cascaded essential nonlinear stiffness, damping and electromagnetic harvester. We realized a versatile function for suppressing the vibration to a satisfied level, and at the same time, it can harvest energy as much as possible. More interestingly, the vibration suppression performance is further enhanced. This work may pave the way for a new strategy for designing advanced smart multi-functional devices.

2 Electromagnetic damping model

The system under consideration is shown in Fig. 1, which comprises a linear primary oscillator with mass

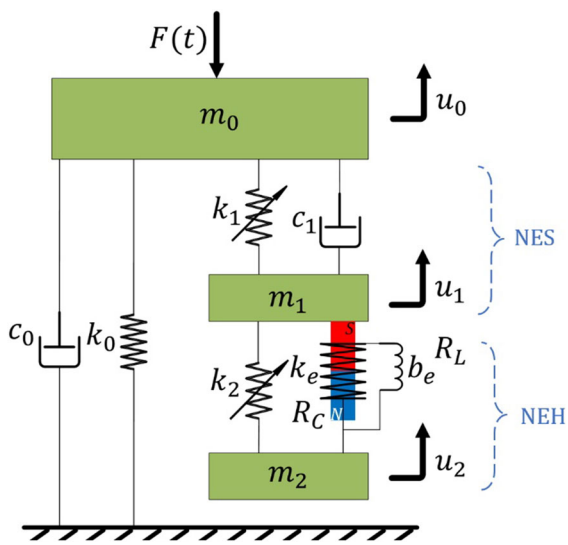

Fig. 1 Mechanical model of the cascaded nonlinear energy sink and energy harvesting system

m_0, damping factor c_0 and stiffness k_0. An integrating system is attached to the primary system, which has two stages, the first one is a nonlinear energy sink and the second one is a nonlinear energy harvester. Both the NES and NEH are designed to possess essential nonlinearities.

The mass, stiffness and damping coefficient of the NES are m_1, k_1 and c_1, respectively. The mass, stiffness and damping coefficient of the NEH are m_2, k_2 and c_2, respectively. Based on Faraday's law, the voltage generated by the coil can be written as

$$V = -\frac{\mathrm{d}\Theta}{\mathrm{d}t} = -N\frac{\mathrm{d}\phi}{\mathrm{d}t} \tag{1}$$

where $\Theta = N\phi$ is the total flux for a N-turn coil. ϕ is the average flux linkage for each turn.

$$\Theta = \sum_{j=1}^{N} \int_{A_j} B(A_j)\mathrm{d}A \tag{2}$$

where B is the magnetic field flux density for a given jth turn area A_j. The electromagnetic force described by Lenz's law can be expressed as

$$F_{\mathrm{EM}} = k_{\mathrm{e}}\dot{Q} \tag{3}$$

where $\dot{Q}$ denotes the current in the coil. The transduction factor k_{e} with respect to the magnetic field flux density and coil size is used to represent the strength of the electromechanical coupling

$$k_{\mathrm{e}} = \frac{\mathrm{d}\Theta}{\mathrm{d}w} \tag{4}$$

where $w = u_2 - u_1$ is the relative displacement between the primary system and the energy harvester. Substituting Eq. (4) into Eq. (1), the electromotive force leads to

$$V = k_{\mathrm{e}}\dot{w}. \tag{5}$$

Substituting Eq. (2) into Eq. (4), based on the assumption of a uniform flux density over the area of the coil, the transduction factor can be expressed as

$$k_{\mathrm{e}} = \frac{Lh(r_0 - r_{\mathrm{i}})}{A_{\mathrm{c}}}B \tag{6}$$

where h is the axial length of the coil, L is the length of the wire, and $A_c = \pi(r_0^2 - r_i^2)$ is the cross-sectional area of the coil. r_0 is the outer radius and r_{i} is the inner radius.

According to the Kirchhoff's law, the current in the circuit due to the electromotive force can be described as

$$k_{\mathrm{e}}(\dot{u}_2 - \dot{u}_1) = L_{\mathrm{c}}\ddot{Q} + (R_{\mathrm{c}} + R_{\mathrm{L}})\dot{Q} \tag{7}$$

where R_{c} is the resistance of the coil and R_{L} is the inductance. The current in the system can be expressed as

$$\dot{Q} = \frac{k_{\mathrm{e}}}{R_{\mathrm{c}} + R_{\mathrm{L}}}(\dot{u}_2 - \dot{u}_1) - \frac{L_{\mathrm{c}}}{R_{\mathrm{c}} + R_{\mathrm{L}}}\ddot{Q}. \tag{8}$$

According to the estimate for the coil inductance provided by Wheeler [29],

$$L_{\mathrm{c}} = \frac{(7.875 \times 10^{-6})(r_0 + r_{\mathrm{i}})^2}{13r_0 - 7r_{\mathrm{i}} + 9h}. \tag{9}$$

The coil impedance can be negligible relative to the load resistance [29, 30]. According to this assumption, Eq. (8) is expressed as

$$\dot{Q} = \frac{k_{\mathrm{e}}}{R_{\mathrm{c}} + R_{\mathrm{L}}}(\dot{u}_2 - \dot{u}_1) = \frac{b_{\mathrm{e}}}{k_{\mathrm{e}}}(\dot{u}_2 - \dot{u}_1) \tag{10}$$

where the expression of the electromagnetic damping b_{e} leads to

$$b_{\mathrm{e}} = \frac{k_{\mathrm{e}}^2}{R_{\mathrm{c}} + R_{\mathrm{L}}}. \tag{11}$$

According to Eq. (8), the electromagnetic force expressed by Eq. (3) can be expressed as

$$F_{\mathrm{EM}} = b_{\mathrm{e}}(\dot{u}_2 - \dot{u}_1). \tag{12}$$

3 Governing equations

Figure 2 shows the schematic representation of the presented energy harvester. The governing equations can be derived based on the Newton's second law:

$$m_0\ddot{u}_0 + c_0\dot{u}_0 + k_0u_0 + k_1(u_0 - u_1)^3 + c_1(\dot{u}_0 - \dot{u}_1) = F(t) \tag{13a}$$

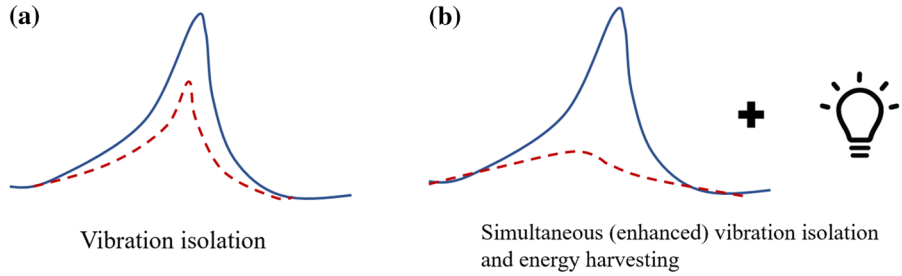

Fig. 2 Comparison between traditional vibration isolation strategy (**a**) and the present system (**b**)

$$m_1\ddot{u}_1 - k_1(u_0-u_1)^3 - c_1(\dot{u}_0-\dot{u}_1) + b_e(\dot{u}_1-\dot{u}_2) + k_2(u_1-u_2)^3 = 0 \tag{13b}$$

$$m_2\ddot{u}_2 + b_e(\dot{u}_2-\dot{u}_1) + k_2(u_2-u_1)^3 = 0 \tag{13c}$$

$$\dot{Q} - \frac{b_e}{k_e}(\dot{u}_2-\dot{u}_1) = 0. \tag{13d}$$

The NES and NEH in Eq. (13) are cascaded essentially nonlinear device for instantaneous energy harvesting and vibration suppression. The essential nonlinearities considered in this work are composed of weakly coupled, linear and essentially nonlinear (nonlinearizable) components, which are physically realized by geometric nonlinearity. This is the key point of NES system. The essential nonlinearity can capture resonance in a broad frequency regime. Introducing the following transformation

$$u_0 = c_x x_0,\ u_1 = c_x x_1,\ u_2 = c_x x_2,\ t = c_t\tau,\ Q = c_q q, \tag{14}$$

the governing equations can be transformed into normalized form as

$$\ddot{x}_0 + \lambda\dot{x}_0 + x_0 + (x_0-x_1)^3 + \eta(\dot{x}_0-\dot{x}_1) = \gamma f(\tau) \tag{15a}$$

$$\mu\ddot{x}_1 - (x_0-x_1)^3 - \eta(\dot{x}_0-\dot{x}_1) + \mu\beta(\dot{x}_1-\dot{x}_2) + \alpha(x_1-x_2)^3 = 0 \tag{15b}$$

$$\varepsilon\ddot{x}_2 + \beta(\dot{x}_2-\dot{x}_1) + \frac{1}{\mu}\alpha(x_2-x_1)^3 = 0 \tag{15c}$$

$$\dot{q} - \beta(\dot{x}_2-\dot{x}_1) = 0. \tag{15d}$$

Here, we introduce the following dimensionless parameters

$$c_t = \sqrt{\frac{m_0}{k_0}}, c_x = \sqrt{\frac{k_0}{k_1}}, c_q = \frac{m_1k_0}{k_e}\sqrt{\frac{1}{k_1m_0}}, \mu = \frac{m_1}{m_0}, \lambda = \frac{c_0}{\sqrt{m_0k_0}}, \eta = \frac{c_1}{m_0}\sqrt{\frac{m_0}{k_0}}, \varepsilon = \frac{m_2}{m_1}, \beta = \frac{b_e}{m_1}\sqrt{\frac{m_0}{k_0}}, \alpha = \frac{k_2}{k_1}, \gamma = \frac{1}{k_0}\sqrt{\frac{k_1}{k_0}}. \tag{16}$$

The energy damped by NES is defined by

$$E_{\mathrm{NES}}(\%) = 100 \times \frac{\eta\int_0^\tau(\dot{x}_1(\tau)-\dot{x}_0(\tau))^2\mathrm{d}\tau}{0.5\times X^2}. \tag{17}$$

The energy harvesting efficiency can be expressed as

$$E(\%) = 100 \times \frac{\frac{k_e^2-R_cb_e}{k_e^2}\int_0^\tau\frac{\mu}{\beta}\dot{q}(\tau)^2\mathrm{d}\tau}{0.5\times X^2} \tag{18}$$

which can be used to evaluate the performance of the present device.

4 Numerical results and discussion

Detailed numerical discussions are carried out in this section to study the nonlinear transient energy transfer. Here, we choose the following system parameters: $\mu = 0.04$, $\beta = 0.1$, $\lambda = 0.01$, $\eta = 0.1$, $\varepsilon = 1$, $\alpha = 0.1$. A single impulsive forcing excitation is applied to the primary system, which can be expressed as $\gamma f(\tau) = X\delta(\tau)$ at $\tau = 0$.,where $\delta(\tau)$ is the Dirac delta function and X is the magnitude of the impulse. It is noted that the nonlinear coefficients are different, resulting in a soft and stiffness.

Figure 3 shows the transient response of the primary system with four input energy levels. In

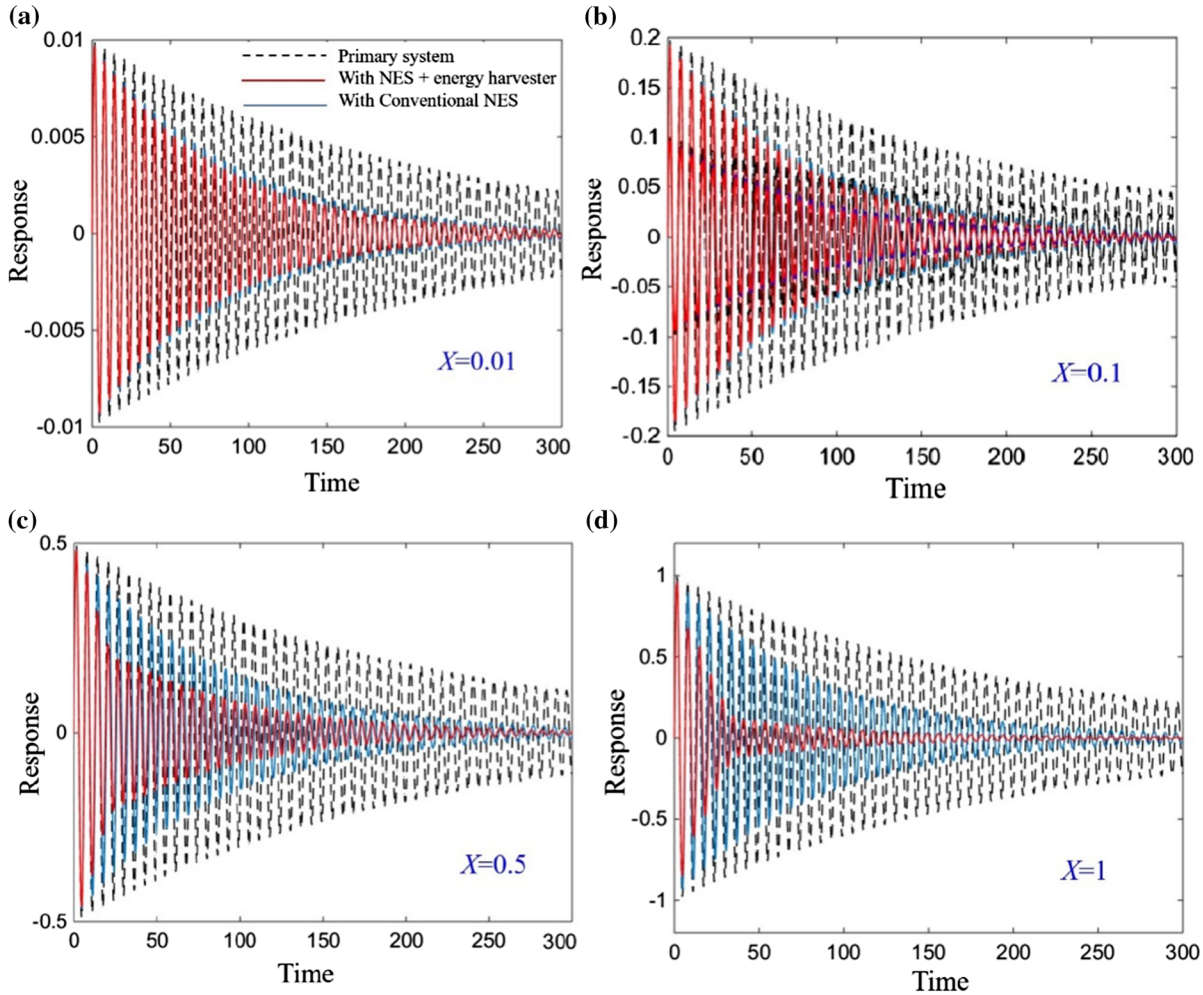

Fig. 3 Comparative performance of the conventional NES and the present system

Fig. 3a, an extremely low impulse $X = 0.01$ is imposed and the dashed black line denotes the response of the primary system without NES–NEH system, which decays as time increases due to the damping c_0. When a single NES is attached, the response is reduced, as depicted in red solid line. In comparison, the NES–NEH system is coupled and a slight reduction is achieved. If the impulse increases to 0.1, 0.5 and 1, as shown in Fig. 3b–d, similar vibration reduction can be achieved and we found that response can be further reduced for the case $X = 0.5$ and $X = 1$.

Figure 4a shows the transient dynamics of the primary system by dimensionless displacements response, NES and NEH for $X = 1$. Figure 4b–d depicts the corresponding wavelet transformation spectra. It is seen that the energy transfer takes place around the fundamental dimensionless frequency $\omega = 1$, which suggests the energy harvesting and absorbing through 1:1 resonance. The intensive energy exchanging occurs within $\tau < 25$, showing a highly efficient one-way energy channeling. This feature means that the designed NES–NEH system is capable of collecting energy in a faster way. The physical reason behind this observed phenomenon is that the asymmetric inertias design of the NES ($\mu = 0.04$) and NEH ($\varepsilon = 1$) permits cascaded 3:1 and 1:1 transient resonance captures in their essentially nonlinear components which, in turn, broadens the frequency range of effective TET and reduces the threshold of the impulse. The NEH can be regarded like an additional local resonator, introducing strong

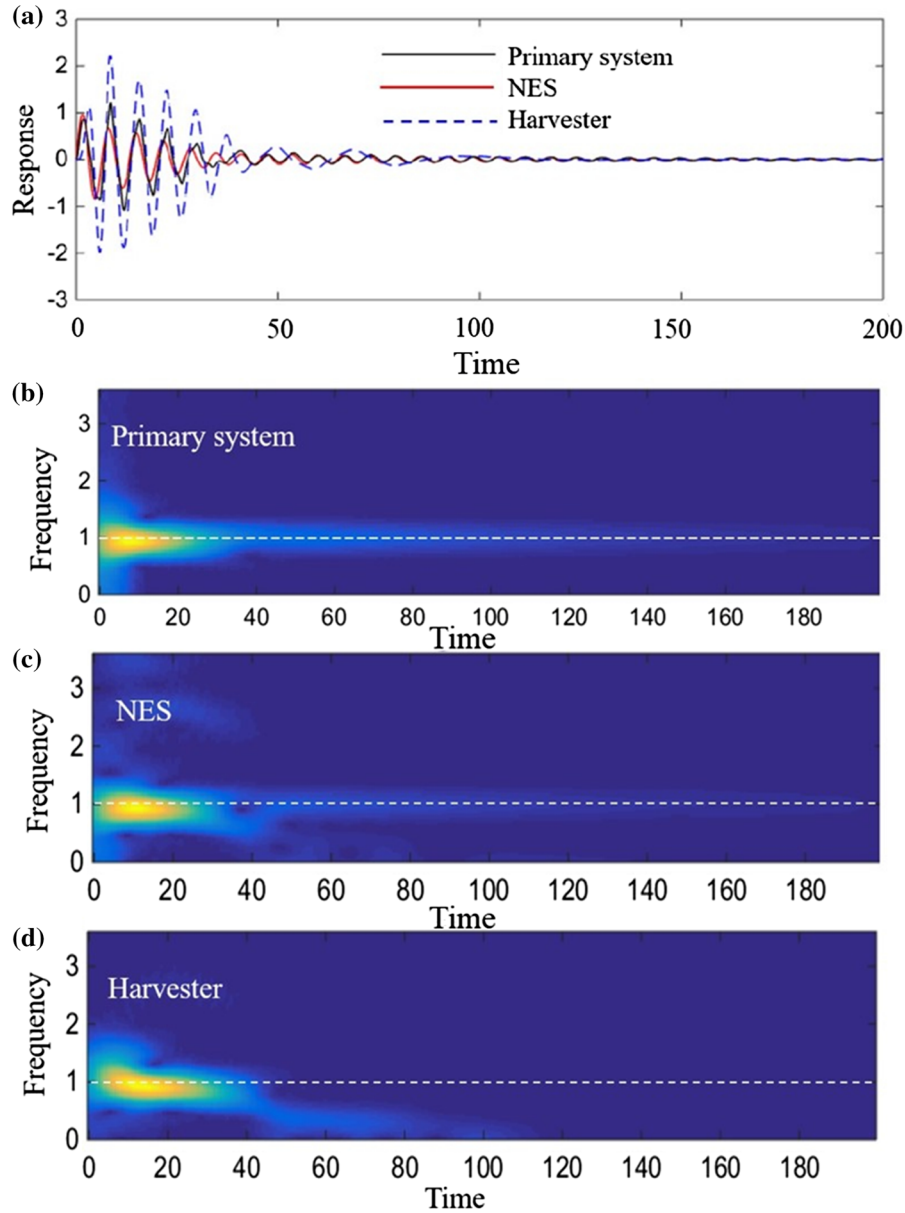

Fig. 4 Transient responses of the present system and the corresponding wavelet transform spectra for $X = 1$

asymmetry, like the concept of mass-in-mass metamaterial device.

Figure 5a, c depicts the simulation results for the relative displacements between the primary system, NES and NEH for $X = 0.01$. Figure 5b, d shows the corresponding wavelet transformation spectra. It is shown that the TET does takes place. The energy is damped by NES and absorbed by NEH. It is noted that $X = 0.01$ is an extremely low impulse; in general, this is below the threshold of conventional NES. Figure 6 shows the results of a higher initial energy level ($X = 1$). The TET occurs as expected; the energy channeling takes place with a much faster way, suggesting an enhanced performance for simultaneous energy harvesting and vibration suppression. Figure 7 shows the simulation for a larger initial energy level $X = 5$. The TET still occurs but takes more time ($t < \sim 190$) to channel the energy. Moreover, the wavelet transformation spectra explore that the TET does not only engage in 1:1 resonance, but also the high-frequency resonance capture takes place, as shown in Fig. 7b, d. This confirms the wide-band

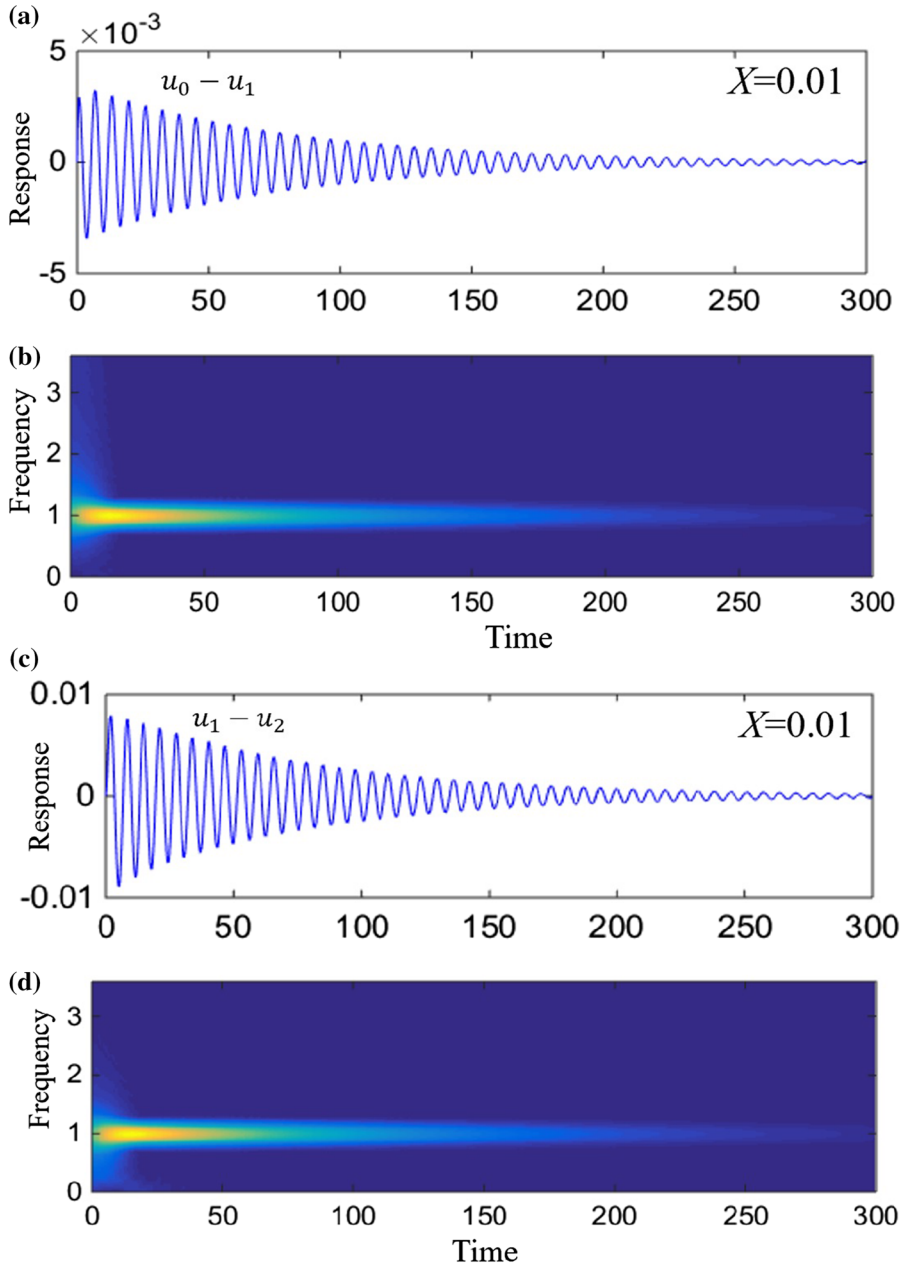

Fig. 5 Transient responses of the present system and the corresponding wavelet transform spectra for $X = 0.01$

performance of our device. In comparing with previous case $X = 0.01$ and $X = 1$, we conclude that the NES–NEH system has a best performance range. This is a typical phenomenon of nonlinear oscillating system.

In order to quantitatively illustrate the phenomenon of TET, we plot energy portion of the case $X = 1$ in Fig. 8. It is shown that the NES absorbs most of the total vibration energy ($\sim 78\%$), while the NEH harvests nearly 9% of the total vibration energy; the primary system damps 11% of the total vibration energy. As a result, the energy remaining in the primary system rapidly drops within $\tau < 38$. It should be stressed that the energy harvesting efficiency is not high, as the primary objective of the NES–NEH design is to guarantee the vibration suppression performance first. Then, NES–NEH can harvest electric energy as much as possible.

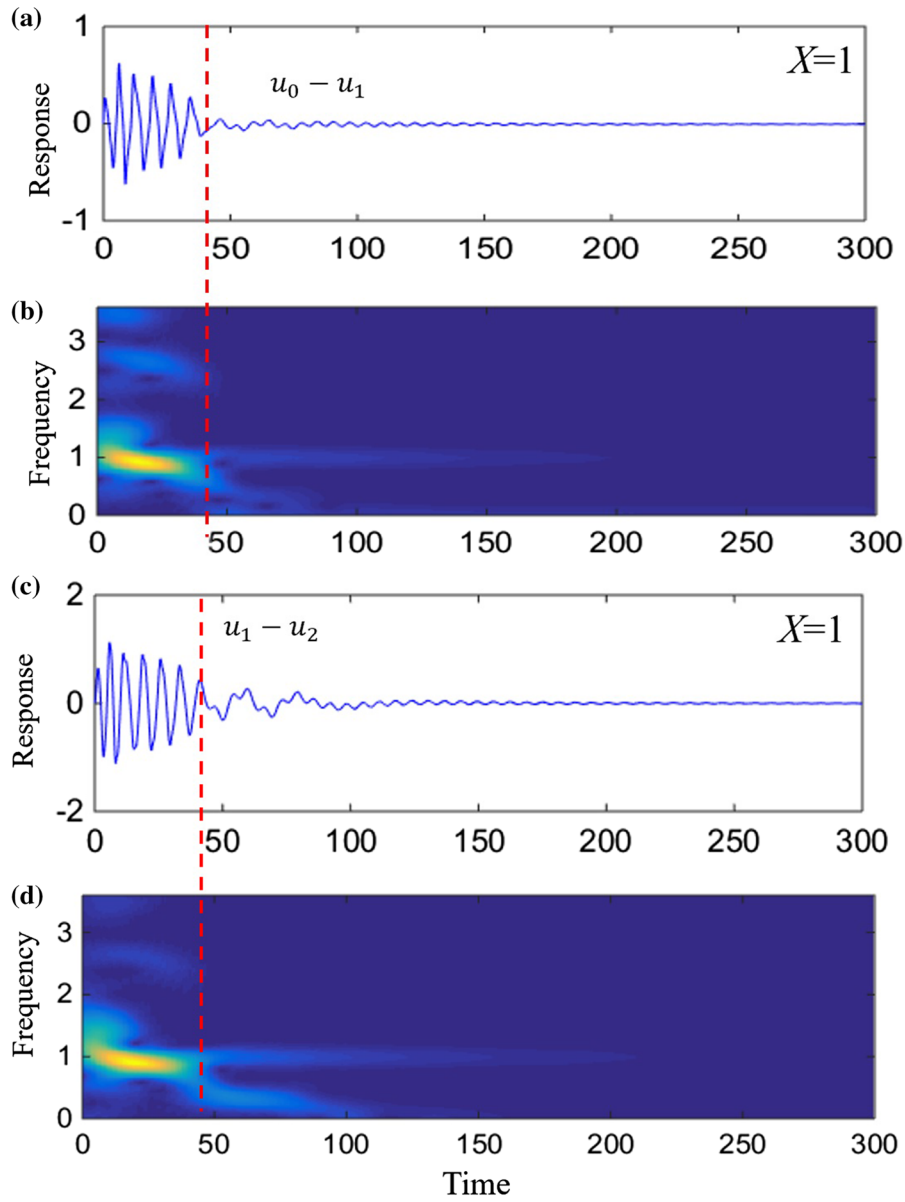

Fig. 6 Transient responses of the present system and the corresponding wavelet transform spectra for $X = 1$

Figure 9 compares the energy efficiency for the primary system with and without the NES or NEH. Clearly, for a primary system, the energy slowly decreases due to damping dissipation. In comparison, a better vibration suppression is observed for the integrated NES–NEH system.

The dependence of energy level of NES–NEH on the impulse magnitude is plotted in Fig. 10a. It is shown that the NES–NEH has a best performance range; for $X = 1$, the NES–NEH device reaches the highest efficiency, where it dissipates $\sim$ 86% of the input energy. It is noted that our system still can dissipate 58% of the input energy for very low impulse level, which is much higher than a single NES system. Figure 10b shows the dependence of energy level of NES–NEH on the parameter α. It is seen that the variation of α has almost neglectable effect on performance of NES–NEH. The energy level remains at $\sim$ 86% as α changes from 0 to 1.

The influence of parameter η is examined in Fig. 11a. It shows that η has a significant influence on energy level of NES–NEH for $\eta = 0 \sim 0.15$. As η

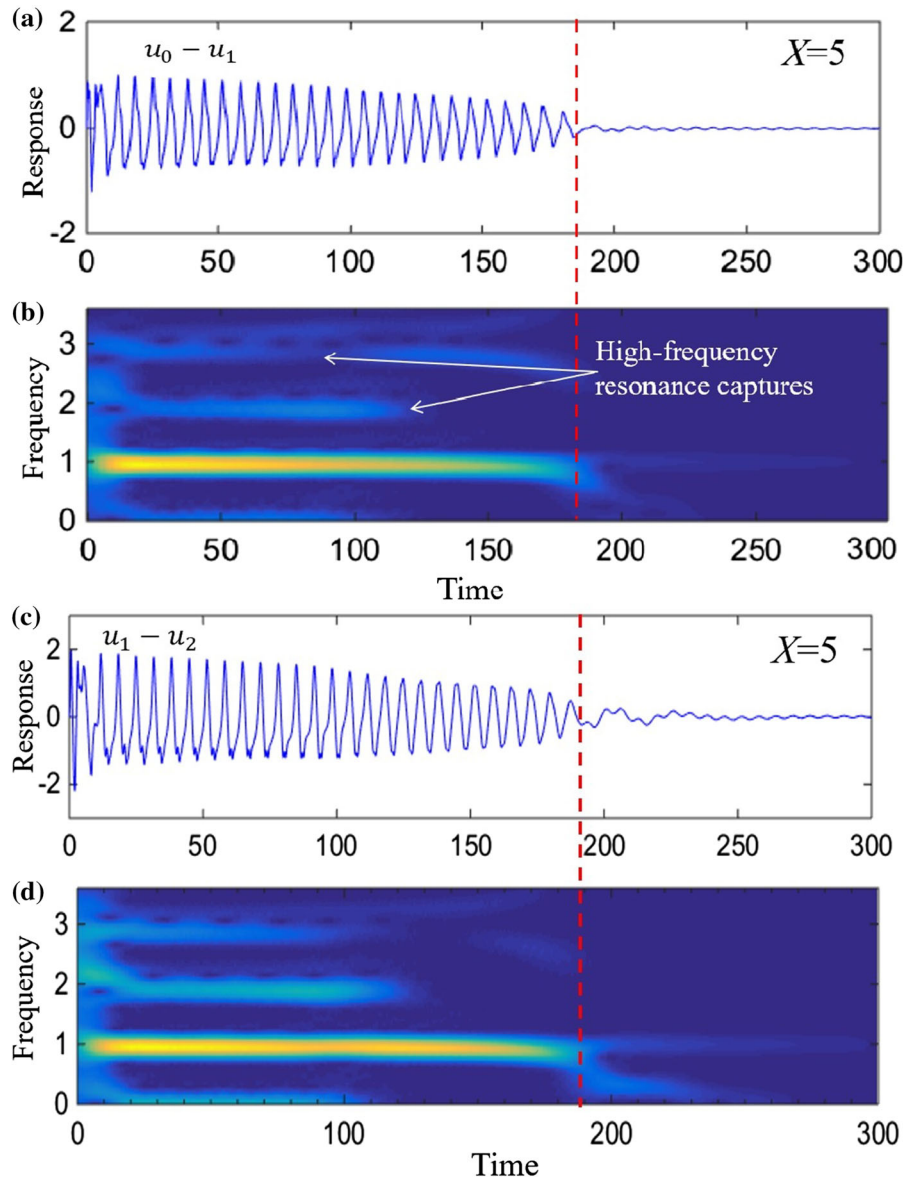

Fig. 7 Transient responses of the present system and the corresponding wavelet transform spectra for $X = 5$

continuously increases from 0.15 to 1, the energy level always remains in a high level $> 82\%$.

The effect of β is discussed in Fig. 11b; it is observed that the energy level decreases from 90 to $\sim$ 70% as βincreases from 0 to 1. That indicates that the NES–NEH system has a best performance if the electromechanical damping coefficient is zero. However, that is impossible due to the inherent resistance of the coil.

5 Conclusions

A cascaded essentially nonlinear system is presented to stabilize a primary system for simultaneously reducing the vibration to a satisfied level and, at the same time, harvesting the energy. The NES–NEH system is realized by integrating two essentially nonlinear stiffnesses, a mechanical damper and an electromechanical damper. The coupled governing equation is a high-dimensional ordinary differential system. Numerical simulation is used to examine the

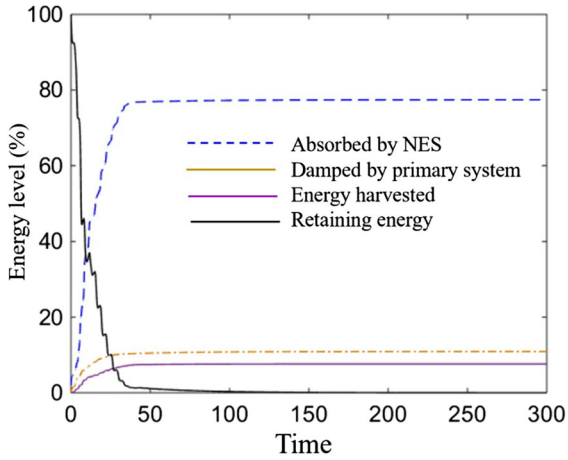

Fig. 8 Percentage of the total energy absorbed by NES, primary system and harvester

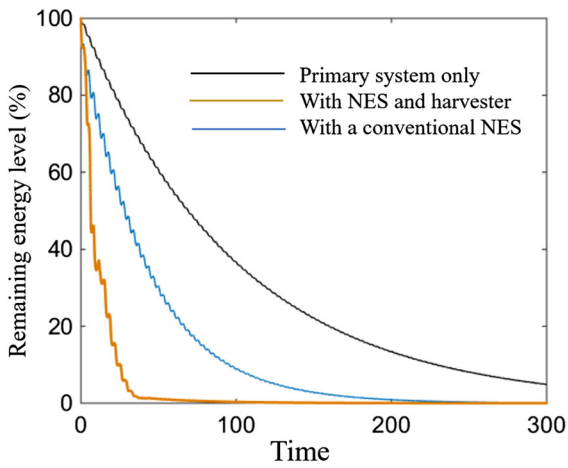

Fig. 9 Percentage of the total energy harvested by the essentially nonlinear energy harvester

effectiveness of the idea. The main result and conclusion are given as follows:

(1) The NES–NEH system is highly effective, which can suppress the vibration to a satisfied low level and generate additional electric energy at the same time. Results show that the vibration suppression performance is superior to a single NES.

(2) For a relatively low applied impulse, the NES–NEH system is proved to be highly effective, which can rapidly dissipate and harvest vibration in ambient for very low amplitude. In comparison, in such a situation, most of the conventional nonlinear oscillators act like linear resonators.

It is found that the NES–NEH system engages in TET via 1:1 resonance capture for small initial energy level, while it absorbs and harvests energy via high-frequency resonance capture for high initial energy level. This is because the asymmetric inertias design of the NES and NEH permits cascaded 3:1 and 1:1transient resonance captures. The NEH can be regarded as an additional local resonator, introducing strong asymmetry like a mass-in-mass nonlinear device.

(3) Due to inherent electromechanical damping coefficient of NEH, the NES–NEH efficiency decreases. It is not avoidable; the smaller electromechanical damping coefficient is preferred in design.

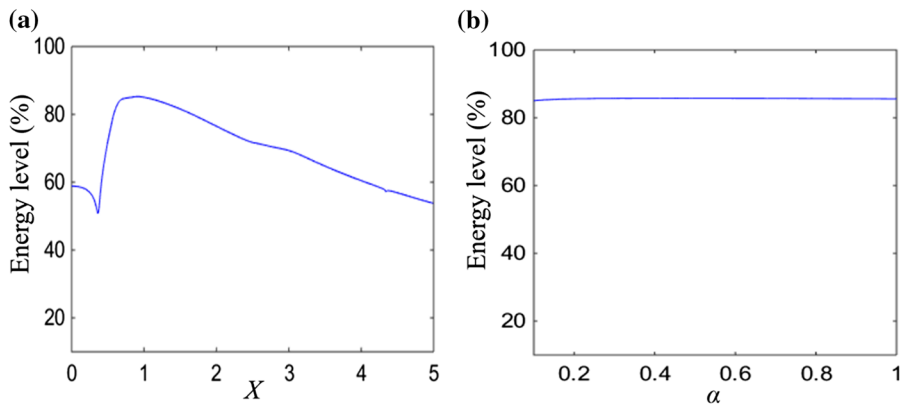

Fig. 10 Effect of external impulse level X and parameter α

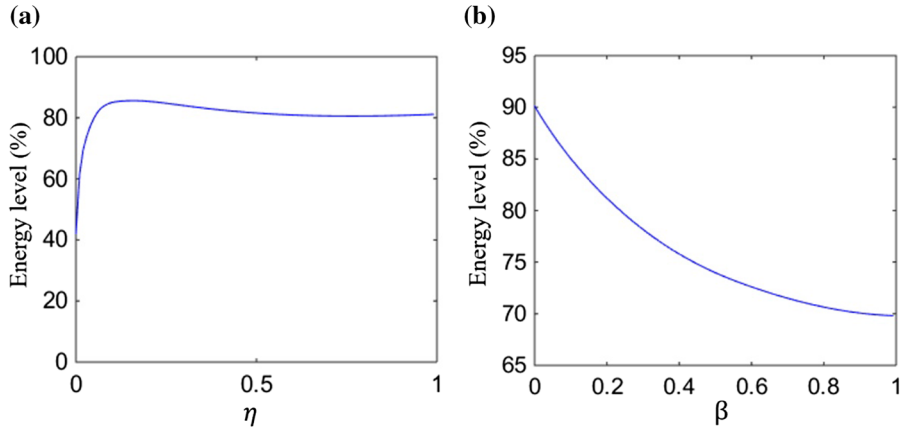

Fig. 11 Effect of parameters η and β

The cascaded nonlinear NES–NEH system unveils new possibilities for energy harvesting and vibration with high efficiency, which may find the applications in smart structures and passive control.

Acknowledgements This work is supported by the National Natural Science Foundation of China (No. 12072221, 11672187) and Scientific Research Project of Tianjin Education Commission (No. 2019KJ121).

Compliance with ethical standards

Conflict of interest The authors declare that they have no conflict of interest.

References

1. Lu, Z.Q., Chen, L.Q., Brennan, M., Yang, T.J., Ding, H., Liu, Z.G.: Stochastic resonance in a nonlinear mechanical vibration isolation system. J. Sound Vib. **370**, 221–229 (2016)
2. Virgin, L.N., Santillan, S.T., Plaut, R.H.: Vibration isolation using extreme geometric nonlinearity. J. Sound Vib. **315**(3), 21–731 (2008)
3. Sun, X.T., Jing, X.J.: Multi-direction vibration isolation with quasi-zero stiffness by employing geometrical nonlinearity. Mech. Syst. Signal Process. **62–63**, 149–163 (2015)
4. Peng, Z.K., Meng, G., Lang, Z.Q., Zhang, W.M., Chu, F.L.: Study of the effects of cubic nonlinear damping on vibration isolations using Harmonic Balance Method. Int. J. Non-Linear Mech. **47**(10), 1073–1080 (2012)
5. Gendelman, O., Manevitch, L.I., Vakakis, A.F., M'closkey, R.: Energy pumping in nonlinear mechanical oscillators: part I—dynamics of the underlying Hamiltonian systems. J. Appl. Mech. **68**(1), 34–41 (2001)
6. Vakakis, A.F., Gendelman, O.: Energy pumping in nonlinear mechanical oscillators: part II—resonance capture. J. Appl. Mech. **68**(1), 42–48 (2001)
7. Dai, H.L., Abdelkefi, A., Wang, L.: Vortex-induced vibrations mitigation through a nonlinear energy sink. Commun. Nonlinear Sci. Numer. Simul. **42**, 22–36 (2018)
8. Bab, S., Khadem, S.E., Shahgholi, M., Abbasi, A.: Vibration attenuation of a continuous rotor-blisk-journal bearing system employing smooth nonlinear energy sinks. Mech. Syst. Signal Process. **84**, 128–157 (2017)
9. Tehrani, G.G., Dardel, M.: Mitigation of nonlinear oscillations of a Jeffcott rotor System with an optimized damper and nonlinear energy sink. Int. J. Non-Linear Mech. **98**, 122–136 (2018)
10. Yang, T.Z., Yang, X.D., Li, Y., Fang, B.: Passive and adaptive vibration suppression of pipes conveying fluid with variable velocity. J. Vib. Control **20**, 1293–1300 (2014)
11. Yang, K., Zhang, Y.W., Ding, H., Yang, T.Z., Li, Y., Chen, L.Q.: Nonlinear energy sink for whole-spacecraft vibration reduction. J. Vib. Acoust. **139**(2), 021011 (2017)
12. Sun, Y.-H., Zhang, Y.W., Ding, H., Chen, L.Q.: Nonlinear energy sink for a flywheel system vibration reduction. J. Sound Vib. **429**, 305–324 (2018)
13. Zhang, Y.W., Zhang, Z., Chen, L.Q., Yang, T.Z., Fang, B., Zang, J.: Impulse-induced vibration suppression of an axially moving beam with parallel nonlinear energy sinks. Nonlinear Dyn. **82**(1–2), 61–71 (2015)
14. Chiacchiari, S., Romeo, F., McFarland, D.M., Bergman, L.A., Vakakis, A.F.: Vibration energy harvesting from impulsive excitations via a bistable nonlinear attachment. Int. J. Non-Linear Mech. **94**, 84–97 (2017)
15. Kremer, D., Liu, K.F.: A nonlinear energy sink with an energy harvester: harmonically forced responses. J. Sound Vib. **410**, 287–302 (2017)
16. Zhou, S.X., Zuo, L.: Nonlinear dynamic analysis of asymmetric tristable energy harvesters for enhanced energy harvesting. Commun. Nonlinear Sci. Numer. Simul. **61**, 271–284 (2018)
17. Zhou, S.X., Cao, J., Inman, D.J., Lin, J., Liu, S.S., Wang, Z.: Broadband tristable energy harvester: modeling and experiment verification. Appl. Energy **133**, 33–39 (2014)
18. Naseer, R., Dai, H.L., Abdelkefi, A., Wang, L.: Piezomagnetoelastic energy harvesting from vortex-induced vibrations using monostable characteristics. Appl. Energy **203**, 142–153 (2017)

19. Jiang, W.A., Chen, L.Q.: Snap-through piezoelectric energy harvesting. J. Sound Vib. **333**(18), 4314–4325 (2014)
20. Zhang, Y., Tang, L.H., Liu, K.F.: Piezoelectric energy harvesting with a nonlinear energy sink. J. Intell. Mater. Syst. Struct. **28**, 307–322 (2016)
21. Izadgoshasb, I., Lim, Y.Y., Lake, N., Tang, L.H., Padilla, R.V., Kashiwao, T.: Optimizing orientation of piezoelectric cantilever beam for harvesting energy from human walking. Energy Convers. Manag. **161**, 66–73 (2019)
22. Wang, H.Y., Tang, L.H.: Modeling and experiment of bistable two-degree-of-freedom energy harvester with magnetic coupling. Mech. Syst. Signal Process. **86**, 29–39 (2017)
23. Gendelman, O.V., Sapsis, T., Vakakis, A.F., Bergman, L.A.: Enhanced passive targeted energy transfer in strongly nonlinear mechanical oscillators. J. Sound Vib. **330**, 1–8 (2011)
24. AL-Shudeifat, M.A.: Highly efficient nonlinear energy sink. Nonlinear Dyn. **76**, 1905 (2014)
25. Wei, Y.M., Peng, Z.K., Dong, X.J., Zhang, W.M., Meng, G.G.: Mechanism of optimal targeted energy transfer. ASME J. Appl. Mech. **84**(1), 011007-1–011007-9 (2016)
26. Fang, Z.W., Zhang, Y.W., Li, X., Ding, H., Chen, L.Q.: Integration of a nonlinear energy sink and a giant magnetostrictive energy harvester. J. Sound Vib. **391**, 35–49 (2017)
27. Li, X., Zhang, Y.W., Ding, H., Chen, L.Q.: Integration of a nonlinear energy sink and a piezoelectric energy harvester. Appl. Math. Mech. **38**, 1019–1030 (2017)
28. Fang, Z.W., Zhang, Y.W., Li, X., Ding, H., Chen, L.Q.: Complexification-averaging analysis on a giant magnetostrictive harvester integrated with a nonlinear energy sink. ASME J. Vib. Acoust. **140**, 021009 (2018)
29. Wheeler, H.: Simple inductance formulas for radio coils. Proc. IRE **16**, 1398–1400 (1928)
30. Remick, K., Dane, Quinn D., Michael, McFarland D., Bergman, L., Vakakis, A.: High-frequency vibration energy harvesting from impulsive excitation utilizing intentional dynamic instability caused by strong nonlinearity. J. Sound Vib. **370**, 259–279 (2016)